

# Investigation of Transverse Cracks Initiation in Continuous Steel Casting Using a Finite Element Approach

S. Castagne<sup>1</sup>, A.M. Habraken<sup>2</sup>

## Summary

A numerical model for steel at elevated temperature which is based on a mesoscopic finite element approach is presented. The objective of the research is the analysis of damage evolution in the material using information from the macroscopic and microscopic scales. As a final application our results are used to study the industrial process of continuous casting of low carbon steel.

## Introduction

To study initiation and propagation of transverse cracks in continuous casting (CC) of low carbon steel a mesoscopic damage model has been developed. This particular type of cracks, which are intergranular, initiates during the bending and unbending phases of the process. These cracks appear by grain boundary cavitation and grain boundary sliding.

The current research studies steel at high temperature (from 1100°C to 800°C) and aims at modelling damage using a numerical mesoscopic approach identified by experimental measurements obtained from the microscopic and macroscopic scales. The developed constitutive laws and finite elements are implemented in a non-linear finite element code developed in the University of Liège.

The first step of the mathematical model development is the definition of a representative mesoscopic cell which is loaded by stress and strain fields determined at macroscopic scale. Such an approach allows the identification of the mesoscopic damage law from macroscopic experiments. Concerning the application to continuous casting, a macroscopic CC model gives the loading (stress, strain and temperature fields) to apply to the mesoscopic cell.

## Mesoscopic cell

In order to represent intergranular creep fracture, the present model contains two-dimensional (2D) finite elements for the grains and one-dimensional (1D) interface elements for their boundaries (see also [1]). Inside the grains, an elasto-visco-plastic law without damage is used, and at its boundaries, a law with damage is preferred.

The grains are modelled by thermomechanical 4-nodes quadrilateral elements of mixed type [2]. Metallographic analysis combining optical microscopy and picric etching on steel samples, have been performed at room temperature to determine the previous austenitic grain size and morphology.

A law of Norton-Hoff type (Eq. 1) is used to quantify the visco-plastic behaviour inside the grain for the studied steel. Its expression in terms of equivalent stress, strain and strain rate is given hereafter:

$$\sigma_e = \epsilon_e^{p_1} \cdot \exp(-p_1 \epsilon_e) \cdot p_2 \cdot \sqrt{3} \cdot (\sqrt{3} \dot{\epsilon}_e)^{p_3} \quad (1)$$

---

<sup>1</sup> M&S Department, University of Liège, Chemin des Chevreuils, 1, bât. B52/3, B-4000 Liège 1, Belgium

<sup>2</sup> FNRS, M&S Department, University of Liège, Chemin des Chevreuils, 1, bât. B52/3, B-4000 Liège 1, Belgium

Compression tests of cylindrical samples have been performed after a thermal treatment that aims at reproducing the thermal cycle of continuous casting. Various strain rates and temperatures have been tested and compared with simulations in order to identify the parameters  $p_1$  to  $p_4$  dependent on temperature in this mechanical law.

The 2D elements modelling the grains are connected by interface elements to account for cavitation and sliding at the grain boundary. As the thickness of the grain boundary is small in comparison with the grain size, the grain boundary can be represented by 1D interface elements. These elements are associated with a constitutive law which includes parameters linked to the presence of precipitates, voids, etc. The damage variable explicitly appears in this law.

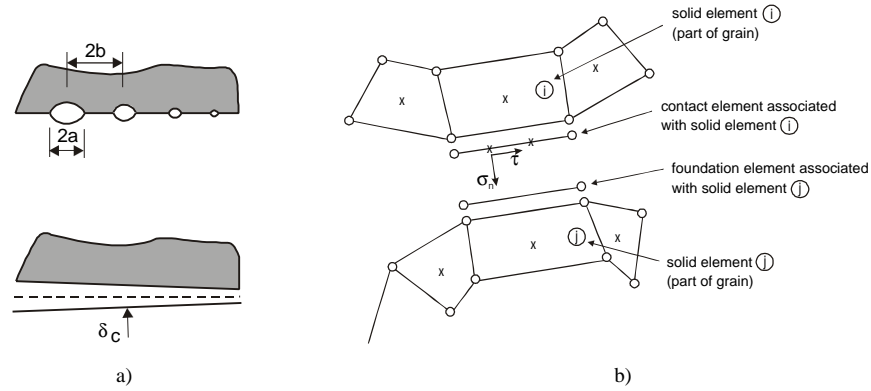


**Figure 1.** a) Discrete and continuous representations of the grain boundary. b) Interface element: contact element, associated foundation, linked solid elements. Dots symbolize nodes and crosses represent integration points.

The interface element is composed of a modified contact element and a foundation element (see figure 1b). For each integration point of the contact element, the program determines the associated foundation segment as well as the solid element to which the foundation is associated. The state variables for the interface element are computed using pieces of information of the two solids elements in contact (elements  $i$  and  $j$  in figure 1b). The state variables in the interface element are the corresponding mean values at the integration points of elements  $i$  and  $j$ .

The original contact element is described in [3] and is usually combined with a Coulomb's friction law. This element has been modified in order to introduce a new interface law and a cohesion criterion. The stress components of the interface element are represented in figure 1b, their evolution is described by the following viscoelastic-type relationships:

$$\dot{\tau} = k_s (\dot{u} - \dot{u}_s) \quad \text{and} \quad \dot{\sigma}_n = k_n (\dot{\delta} - \dot{\delta}_c) \quad (2)$$

This is a penalty method where penalty coefficient  $k_s$  and  $k_n$  are very large to keep the deviations  $(\dot{u} - \dot{u}_s)$  and  $(\dot{\delta} - \dot{\delta}_c)$  small.  $\dot{u}$  and  $\dot{\delta}$  are respectively the relative sliding velocity of adjacent grains due to shear stress  $\tau$  and the average separation rate, normal to the interface, due to damage growth. These variables are directly computed from nodal displacements.  $\dot{u}_s$  and  $\dot{\delta}_c$  are the same variables but related to the damage law. Their evolution are computed in the next section (Eq. 3 and Eq. 13).

### Interface law: evolution of the damage

The relevant damage mechanisms at the mesoscale are viscous grain boundary sliding, nucleation, growth and coalescence of cavities leading to microcracks. The linking-up process subsequently leads to the formation of a macroscopic crack.

Grain boundary sliding is governed by:

$$\dot{u}_s = w \frac{\tau}{\eta_B} \quad (3)$$

where  $\dot{u}_s$  is the relative velocity between two adjacent grains,  $w$  is the thickness of the grain boundary and  $\eta_B$  is the grain boundary viscosity. However in [1],  $\eta_B/w$  is expressed in term of the strain-rate parameter  $\dot{\epsilon}_B$  defined as follows:

$$\dot{\epsilon}_B = \dot{\epsilon}_0 \left( \frac{w \sigma_0}{\eta_B d \dot{\epsilon}_0} \right)^{\frac{n}{n-1}} \quad (4)$$

with  $d$  a length parameter related to the grain size,  $n$  the creep exponent.  $\sigma_0$ ,  $\dot{\epsilon}_0$  are reference stress and strain-rate.

In the context of damage at high temperature, the mechanism of voids nucleation, growth and coalescence is established. In most engineering alloys, cavities have been observed to nucleate continuously. The following experimental relation has been suggested [4]:

$$\dot{N} = \beta \sigma_n^2 \dot{\epsilon}_e^C = F_n \left( \frac{\sigma_n}{\Sigma_0} \right)^2 \dot{\epsilon}_e^C \quad \text{with } \sigma_n \geq 0 \quad (5)$$

where  $N$  is the average number of cavities per unit length of grain boundary,  $\dot{\epsilon}_e^C$  is the effective creep strain rate,  $\sigma_n$  the normal stress, introduced to allow a faster nucleation on those grain boundaries which are perpendicular to the loading direction, and  $\beta$  a material constant. For the second formulation,  $F_n$  is the nucleation parameter of the material and  $\Sigma_0$  a normalization constant.  $F_n$  is the microstructural parameter which influences the nucleation rate at the grain boundary. Through this parameter, we can introduce zones where the nucleation is more important, to take into account the precipitation state for instance. According to Eq. 5, the nucleation will begin with the plastification. Nevertheless, experimentally, nucleation appears sometimes later, that is why we have to introduce a threshold to indicate the beginning of the nucleation. We define the parameter  $S$  which combines the stress and the cumulated strain:

$$S = \left( \sigma_n / \Sigma_0 \right)^2 \dot{\epsilon}_e^C \quad (6)$$

This parameter  $S$  characterizes the state of the material before nucleation. It will grow with the strain and when the threshold value is reached, nucleation begins and the parameter  $S$  has no more utility. To define the threshold value  $S_{thr}$ , we suppose that it is related to a minimum cavity density  $N_l$  from which nucleation can be observed and a factor  $F_n$  indicating the importance of the nucleation activity of the material:

$$S_{thr} = N_1/F_n \quad (7)$$

Finally, experience shows that the cavity density tends to saturate for large creep strains, thus we suppose that nucleation of new cavities stops when  $N$  reaches the value  $N_{max}$ . If  $2b$  is the cavity spacing,  $N$  is related to it by  $N = 1/pb^2$ . We have:

$$\dot{b} = -\frac{1}{2} \frac{\dot{N}}{N} b = -\frac{\pi}{2} b^3 \beta \sigma_n^2 \dot{\epsilon}_e^C \quad (8)$$

The nucleation rate  $\dot{N}$  is related to the internal state of the material  $N$  as well as to the stress  $\mathbf{s}_n$  and strain rate  $\dot{\epsilon}_e^C$  states on the grain boundary. With a one-dimensional element, this nucleation rate  $\dot{N}$  can be interpreted as a measure of the rate of evolution of the cavity spacing  $\dot{b}$ . This equation can be used to compute the decrease rate of  $b$  due to continuous nucleation of cavities.

A detailed formulation of the cavity growth under diffusion and creep deformations can be found in [5]. An idealized formulation of the grain boundary geometry is used: the cavities are supposed to be uniformly distributed with an average spacing of  $2b$  and a diameter of  $2a$  (see figure 1a). For the proposed idealized boundary geometry with a cavity tip angle  $\Psi$ , the cavity growth rate is:

$$\dot{a} = \dot{V} / [4\pi a^2 h(\Psi)] = (\dot{V}_1 + \dot{V}_2) / [4\pi a^2 h(\Psi)] \quad (9)$$

where  $h(\Psi) = [(1 + \cos \Psi)^{-1} - 0.5 \cos \Psi] / \sin \Psi$  (shape function of the cavity) and  $\dot{V}$  is the total cavity volume growth rate, which is divided into diffusion growth  $\dot{V}_1$  and creep deformation  $\dot{V}_2$ :

$$\dot{V}_1 = 4\pi D \frac{\sigma_n}{\ln(1/f) - (3-f)(1-f)/2} \quad (10)$$

$$\dot{V}_2 = \begin{cases} -2\pi \dot{\epsilon}_e^C a^3 h(\Psi) \left( \frac{3}{2n} \left| \frac{\sigma_m}{\sigma_e} \right| + \frac{(n-1)(n+0.4319)}{n^2} \right)^n & \text{for } \frac{\sigma_m}{\sigma_e} < -1 \\ 2\pi \dot{\epsilon}_e^C a^3 h(\Psi) \left( \frac{3}{2n} + \frac{(n-1)(n+0.4319)}{n^2} \right)^n & \text{for } \left| \frac{\sigma_m}{\sigma_e} \right| \leq 1 \\ 2\pi \dot{\epsilon}_e^C a^3 h(\Psi) \left( \frac{3}{2n} \frac{\sigma_m}{\sigma_e} + \frac{(n-1)(n+0.4319)}{n^2} \right)^n & \text{for } \frac{\sigma_m}{\sigma_e} > 1 \end{cases} \quad (11)$$

where  $D$  is a constant related to the material diffusion,  $n$  the creep exponent,  $\mathbf{s}_n$ ,  $\mathbf{s}_e$  and  $\mathbf{s}_m$  are respectively the normal, effective, and mean stresses applied on the grain boundary. The variable  $f$  is defined as follows:

$$f = \max \left\{ (a/b)^2, \left[ a / (a + 1.5L) \right]^2 \right\} \text{ where } L = (D \sigma_e / \dot{\epsilon}_e^C)^{1/3} \quad (12)$$

The coupling between diffusive and creep contribution to void growth is introduced through the length scale  $L$ : for small values of  $a/L$ , cavity growth is dominated by diffusion while for larger values, creep growth becomes more and more important. Finally the discrete cavity distribution is replaced by a continuous distribution on each facet of the grain boundary so that the cavity volume  $V$  and the average separation between two grains  $d_c$  evolve in a continuous way on the facet (see figure 1a). Then, the separation rate is given by:

$$\dot{\delta}_c = \frac{\dot{V}}{\pi b^2} - \frac{2V}{\pi b^2} \frac{\dot{b}}{b} \quad (13)$$

Coalescence takes place when cavities are sufficiently close to each other to collapse. At this moment, the crack begins to propagate and the interface elements are no more in contact. The parameter used to define the coalescence activation is the ratio  $a/b$ . We call it a damage variable in the current model. When this ratio reaches a critical threshold, coalescence is triggered and crack appears.

### Meso-macro link

A macroscopic continuous casting model [6] is available in the University of Liège. This model provides various results such as temperature fields, thickness of the solidified shell, stress, strain and strain rate fields in the strand. It also computes some crack risk indicators but does not integrate a coupled damage approach.

With the mesoscopic model, a coupled damage approach is proposed. As we want to analyse the process at the grain scale, we have to concentrate on specific zones. Thanks to the macroscopic model, we know the critical zones to take into account and the loading to apply to the mesoscopic cell. Experiments and macroscopic modelling show that transverse cracks always appear near the edge of the slab and at its surface, the mesoscopic cell is chosen in this zone.

The mesoscopic cell is surrounded by a transition zone which allows the transfer of data from the macroscopic model (see figure 2a). It is important to follow the whole process as we use elasto-viscoplastic constitutive laws. The history of displacements known thanks to the macroscopic simulation is imposed on each node of the boundary of the transition zone. With these boundary conditions, the crack is free to initiate in the mesoscopic cell.

At each time step, the temperature of each node is fixed according to the results of the macroscopic simulation and no thermal exchange is computed at the mesoscopic scale. All the thermal problem has already been treated in the macroscopic model.

### Results and conclusions

Growth of cracks for the simple loading of figure 2a is simulated as a first application. The parameters for the interface law are issued from [1]. The displacement rate is chosen to obtain strain rates compatible with those usually encountered in continuous casting ( $10^{-3} \text{ s}^{-1}$ ). Application of actual loadings issued from the macroscopic model has still to be done.

The mesh is defined on the basis of a micrograph realised on a low carbon steel. A picric etching was previously done to locate the austenitic grain boundaries. The size of the mesoscopic cell is 5x5 [mm] and it is surrounded by a transition zone (10x15 [mm]). We remark that the austenitic grain size is quite large (diameter  $\approx 1 \text{ mm}$ ).

On figure 2b, we detect two cracks initiating. Figures 2c-e show propagation of cracks along grain boundaries. Stresses concentrate around the crack tip and decrease on the border of the crack. The size of the mesoscopic cell was chosen to analyse the initiation of cracks (figure 2b). With this example, we can also follow their propagation (figures 2c-e) but a larger cell would be necessary to avoid perturbations in the surrounding zone when cracks are propagating. Nevertheless, with this first example, the stability of the code when interface elements are debonding can be analysed.

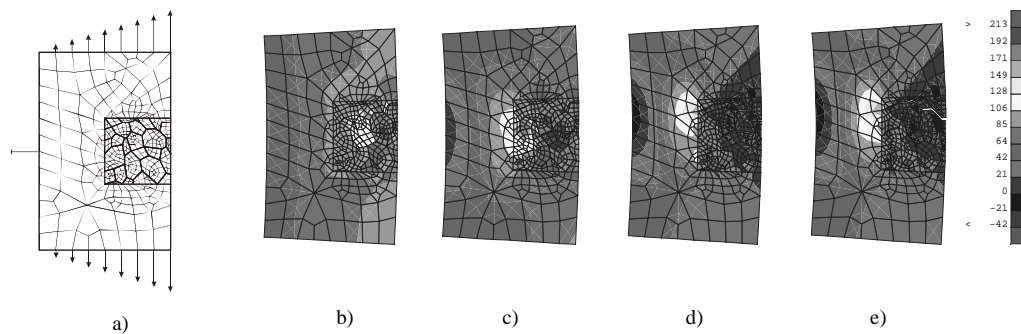


**Figure 2.** a) Imposed displacements. b-e) Stress maps  $s_m$  [Mpa] at different steps of the crack propagation.

The mesoscopic model allows a parametrical study of factors such as grain size, precipitation state or oscillation marks geometry which can not be analyzed with the macroscopic model.

### Acknowledgements

The authors thank the National Fund for Scientific Research of Belgium (FNRS) for its support. Industrial partners ARCELOR and its research teams IRSID and the Technical Direction of Cockerill Sambre are acknowledged.

### References

- 1 P. Onck and E. van der Giessen (1999): "Growth of an Initially Sharp Crack by Grain Boundary Cavitation", *J. Mech. Phys. Solids*, Vol. 47, pp. 99-139.
- 2 Y. Zhu and S. Cescotto (1995): "Unified and Mixed Formulation of the 4-Node Quadrilateral Elements by Assumed Strain Method: Application to Thermomechanical Problems", *Int. J. Num. Meth. Eng.*, Vol. 38, pp. 685-716.
- 3 A.M. Habraken and S. Cescotto (1998): "Contact between Deformable Solids: the Fully Coupled Approach", *Mathl. Comput. Modelling*, Vol. 28, pp. 153-169.
- 4 E. van der Giessen and V. Tvergaard (1994): "Development of Final Creep Failure in Polycrystalline Aggregates", *Acta Metall.*, Vol. 42, pp. 959-973.
- 5 V. Tvergaard (1984): "On the Creep Constrained Diffusive Cavitation of Grain Boundary Facets", *J. Mech. Phys. Solids*, Vol. 32, pp. 373-393.
- 6 F. Pascon and A.M. Habraken (2003): "2D½ Thermo-Mechanical Model of Continuous Steel Casting Using F.E.M.", *Proc. 6<sup>th</sup> Esaform Conference on Metal Forming, Salerno, Italy*.